Stationary bathtub vortices and a critical regime of liquid discharge

YURY A. STEPANYANTS AND GUAN H. YEOH

Reactor Operations, Australian Nuclear Science and Technology Organisation (ANSTO),
Lucas Heights, PMB 1, Menai (Sydney), NSW, 2234, Australia
Yury.Stepanyants@ansto.gov.au

A modified Lundgren model is applied for the description of stationary bathtub vortices in a viscous liquid with a free surface. Laminar liquid flow through the circular bottom orifice is considered in the horizontally unbounded domain. The liquid is assumed to be undisturbed at infinity and its depth is taken to be constant. Three different drainage regimes are studied: (i) subcritical, where whirlpool dents are less than the fluid depth; (ii) critical, where the whirlpool tips touch the outlet orifice; and (iii) supercritical, where surface vortices entrain air into the intake pipe. Particular attention is paid to critical vortices; the condition for their existence is determined and analysed. The influence of surface tension on subcritical whirlpools is investigated. Comparison of results with known experimental data is discussed.

1. Introduction

Whirlpools or bathtub vortices often appear in the course of water drainage, for example, from baths, kitchen sinks, laboratory tanks or industrial reservoirs. In spite of their common occurrence, their structure, formation and subsequent dynamics are still not completely understood and adequately described. Determination of the whirlpool's direction of rotation has been the focus of intense fascination for many years. Experiments have demonstrated that the direction of whirlpool rotation depends on many seemingly random factors. However, under ideal conditions where external factors such as residual fluid motion in the vessel, pressure variations caused by air flow, asymmetry in the initial or boundary conditions, and temperature inhomogeneity are eliminated, whirlpools form under the sole influence of the Coriolis force due to the Earth's rotation (see e.g. Lugt 1983, chap. 3). (Normally, this force is negligibly small in comparison with other random forces.) In accordance with theoretical predictions, experiments have confirmed that vortices tend to rotate counter-clockwise in the northern hemisphere (Turmlitz 1908; Shapiro 1962; Binnie 1964) and clockwise in the southern hemisphere (Trefethen *et al.* 1965). Accurate observations show, however, that the direction of rotation reverses when the vessel is nearly empty, i.e. when the liquid layer becomes very thin in the vessel (Sibulkin 1962, 1983; Binnie 1964; Kelly, Martin & Taylor 1964).

Vortices similar to the bathtub whirlpools are often experienced in nature and engineering devices. For example, intense surface vortices may appear above the water intakes from natural water bodies such as estuaries, lakes, rivers, ponds and storage pools (Knauss 1987; Kocabaş & Yildrim 2000); at turbine intakes (Andrade 1963; Lugt 1983); and in draining large oil reservoirs. However, the appearance of

intense vortices with gaseous cores in industrial and engineering devices, such as in water withdrawal from sumps in emergency core cooling systems of nuclear power stations (Hecker 1981), is highly undesirable because of difficulties associated with the operational efficiency and maintenance of the associated equipment.

Whirlpool formation in the liquid coolant surface at the upper plenum of fast breeder nuclear reactors (Baum 1974; Monji *et al.* 2005) and in the primary cooling systems of conventional thermal nuclear reactors represent other examples of unwanted vortex manifestation in nuclear facilities. Under certain conditions (depending on the coolant circulation rate, coolant depth, diameter of intake pipe, temperature, surface tension and vessel size) whirlpools can exist within the reactor core. These whirlpools draw gas from the top of the vessel into the drainage pipes at the bottom thus resulting in undesirable negative reactivity spikes owing to the presence of gas bubbles. It has been ascertained that even small amounts ($\sim$1% by volume) of air entrainment by surface vortices in a suction pipe can cause significant loss of efficiency (as much as 15% reduction) in a centrifugal pump (see e.g. Chang & Lee 1995). Air concentration greater than 3% by volume has been found to significantly degrade the performance or even result in the damage of the mechanical components of the pump. The study of bathtub vortices is therefore important and topical not only from a purely academic viewpoint, but also for a better understanding of such fluid phenomena in practical engineering systems.

Numerous papers have studied the transient process of rapid formation of a surface dip when the bottom sink is opened quickly (see e.g. Tyvand & Haugen 2005 and references therein). In some cases, bathtub vortices are formed in the course of liquid drainage, whereas in other cases drainage occurs without whirlpool formation. Despite the apparent instability of drainage without whirlpool formation, it has been experimentally realized by Andrade (1963) and Lubin & Springer (1967), at least on a relatively short time scale. It can occur under the preconditions of eliminating any residual motions in the liquid and ensuring negligible external influences caused by a temperature gradient, vessel vibration, air flow, asymmetries in the boundary or initial conditions. In this rotation-free discharge, fluid may either glide to the outlet (with or without dent formation on the surface) or run through the outlet pipe partially occupied by a gaseous core in the centre, or flow through the outlet with the formation of a jet-type hump on a surface above the output orifice (Zhou & Graebel 1990; Forbes & Hocking 1995).

There have been several attempts to construct analytical or numerical solutions describing stationary whirlpools in a fluid with a free surface. One of the intriguing aspects of this problem is the existence of a critical vortex, that is, the vortex whose tip reaches the entrance to the outlet pipe at the bottom of the vessel. The flow regime corresponding to critical vortices divides the situations where vortices of relatively small amplitude exist in the liquid from those where the intense vortices appear with gaseous cores extending into the drainage pipe. One of the first theoretical attempts to quantify the condition for the existence of critical vortices was made by Odgaard (1986; see Gulliver, Paul & Odgaard 1988 for a discussion of this paper). He suggested a model which provided a reasonable relationship between the critical depth of a liquid and other flow parameters (drain-rate, circulation, viscosity and surface tension). Odgaard's model is based on the assumption that the velocity field is described by the Burgers vortex representing the exact solution of hydrodynamic equations for viscous unbounded fluid. However, the velocity field in the bathtub vortex can be approximated by the Burgers vortex only when the free surface is almost planar, that is when the whirlpool dent is small in comparison with the

total fluid depth. Thus, the results obtained by Odgaard (1986) for critical vortices are questionable. Rott (1958) and Miles (1998) constructed approximate analytical solutions for small-dent whirlpools, where the approximation of the velocity field by the Burgers vortex is indeed well founded.

A more consistent theory of stationary whirlpools in a rotating vessel was originally suggested by Lundgren (1985) and subsequently developed further by Andersen *et al.* (2003, 2006) to include the surface tension and bottom upwelling owing to the effect of viscosity in the Ekman boundary layer near the outlet orifice. This modified model designated as the LABSRL-model, was applied to the interpretation of experimental whirlpool data obtained in a rotating cylindrical vessel with water circulating at a given flow rate. By adjusting the two fitting parameters contained in their theory, Andersen *et al.* (2003, 2006) obtained fairly good agreement between their theoretical/numerical results and the experimental data for moderate flow conditions: drain rate through the vessel $Q \sim 1.8 \times 10^{-6}$ m^3 s^{-1} and vessel rotation rate $\Omega \sim 1.26$ rad s^{-1} ($\sim$12 r.p.m.). It was also demonstrated in these experiments that surface tension greatly affected both the whirlpool shape and its dip. In particular, for one of the cases studied, the model without surface tension overestimated the depth of the experimentally observed whirlpool by 70%, whereas the model with surface tension showed good agreement with the experimental data.

Further extension of the model and its validation for whirlpools in non-rotating vessels remain highly desirable. Some development has been undertaken by Lautrup (2005, §26.6) who, however, neglected surface tension for the sake of simplicity.

In the present paper, we apply the LABSRL-like model for the description of stationary whirlpools in a non-rotating vessel while taking into account surface tension. Without surface tension, the present model is capable of describing not only the subcritical regime of discharge, but also critical and even supercritical regimes where the gaseous vortex core occupies some portion of the bottom outlet orifice. Flow parameters producing such vortices are determined numerically, and are analysed. It is shown that the critical vortex shape is determined by three independent parameters: the dimensionless circulation; flow rate through the vessel; and surface tension. The results obtained in this study are found to be in good agreement with those obtained by Odgaard (1986) and other authors.

2. Theory

Consider a stationary liquid flow with a free surface in a cylindrical vessel whose radius is substantially larger than all other characteristic scales so that the liquid may be treated as horizontally unbounded (figure 1). The origin of the cylindrical coordinate system is located at the centre of the bottom orifice, and the z-axis is directed upwards. Liquid discharges through the outlet pipe with a constant volumetric drainrate Q and has an unperturbed Constant depth at 'infinity' of H_0. The governing continuity and Navier–Stokes equations describing stationary whirlpools in a non-rotating vessel are given by the following set of equations:

$$\frac{1}{r}\frac{\partial}{\partial r}(ru_r) + \frac{\partial u_z}{\partial z} = 0, \tag{1}$$

$$u_r\frac{\partial u_r}{\partial r} + u_z\frac{\partial u_r}{\partial z} - \frac{u_\varphi^2}{r} = -\frac{1}{\rho}\frac{\partial p}{\partial r} + \nu\left(\frac{\partial^2 u_r}{\partial r^2} + \frac{1}{r}\frac{\partial u_r}{\partial r} - \frac{u_r}{r^2} + \frac{\partial^2 u_r}{\partial z^2}\right), \tag{2}$$
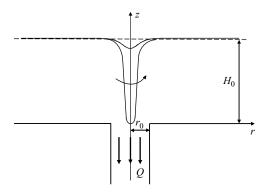
FIGURE 1. Sketch of liquid flow in the cylindrical coordinate system. A small-amplitude whirlpool is shown together with a critical vortex whose dip reaches the entrance to the outlet.

$$u_r \frac{\partial u_\varphi}{\partial r} + u_z \frac{\partial u_\varphi}{\partial z} + \frac{u_r u_\varphi}{r} = \nu \left(\frac{\partial^2 u_\varphi}{\partial r^2} + \frac{1}{r} \frac{\partial u_\varphi}{\partial r} - \frac{u_\varphi}{r^2} + \frac{\partial^2 u_\varphi}{\partial z^2} \right), \tag{3}$$

$$u_r \frac{\partial u_z}{\partial r} + u_z \frac{\partial u_z}{\partial z} = -\frac{1}{\rho} \frac{\partial p}{\partial z} + \nu \left(\frac{\partial^2 u_z}{\partial r^2} + \frac{1}{r} \frac{\partial u_z}{\partial r} + \frac{\partial^2 u_z}{\partial z^2} \right) - g, \tag{4}$$

where u_r, u_z and u_φ are the radial, axial and azimuthal components of the velocity field; g is the acceleration due to gravity; ρ is the fluid density; p is the pressure; and ν is the kinematic viscosity.

2.1. *Simplified analytical approach (Odgaard's model)*

Following Odgaard (1986), the azimuthal component of the velocity can be assumed in the form:

$$u_\varphi = \frac{\Gamma}{2\pi r} f(r), \tag{5}$$

where Γ is the circulation and $f(r)$ is some unknown function. Substituting (5) into (3) yields

$$\nu \frac{d}{dr} \ln \left[\frac{1}{r} \frac{df(r)}{dr} \right] = u_r. \tag{6}$$

For vortices with a small 'amplitude' η (i.e. of a shallow dent) where $\eta \ll H_0$, the axial velocity component u_z in the vicinity of the z-axis can be taken to behave linearly with the vertical coordinate z:

$$u_z(r, z) \approx a(z - H_0), \quad r \leqslant r_0, \quad z \leqslant H_0, \tag{7}$$

where $a > 0$ is the coefficient of proportionality and r_0 is the radius of the orifice. From the continuity equation (1), it follows that the radial velocity component linearly depends on r and is directed towards the axis z:

$$u_r(r, z) \approx -\frac{1}{2}ar, \quad r \leqslant r_0, \quad z \leqslant H_0. \tag{8}$$

Alternatively, the radial velocity for the small-amplitude whirlpool may be assumed to depend on r only and vanish on the z-axis or that the liquid discharge through the cylindrical area of unit height coaxial with z-axis is proportional to the area of the cylinder base as $q_r \sim r^2$. Then, the continuity equation (1) leads to the linear dependence of u_z on z, as represented by (7). All these equivalent assumptions have

been exploited in different papers (see e.g. Einstein & Li 1955; Marris 1966; Odgaard 1986; Lautrup 2005). In essence, (7) and (8) can be treated as representations of the first terms of the truncated Taylor series for the corresponding velocity components. The coefficient a is related to the total drain rate Q through the orifice:

$$Q = 2\pi \int_0^{r_0} u_z(r, 0)r \, \mathrm{d}r = -\pi a H_0 r_0^2, \quad a = \frac{-Q}{\pi H_0 r_0^2}. \tag{9}$$

Note that Q is negative here, which means that the flow is directed downwards.

With $u_r(r, z)$ given by (8), (6) can be solved subject to the boundary conditions: $u_\varphi = 0$ at $r = 0$ and $f(r) \to 1$ when $r \to \infty$. The corresponding solution is:

$$u_\varphi = \frac{\Gamma}{2\pi r} \left[1 - \exp\left(-\frac{a}{4\nu} r^2 \right) \right] \tag{10}$$

with the following asymptotes:

$$u_\varphi \to \begin{cases} \dfrac{a\Gamma}{8\pi\nu} r & \text{when } r \to 0, \\[2mm] \dfrac{\Gamma}{2\pi r} & \text{when } r \to \infty. \end{cases} \tag{11}$$

The above solution known as the Burgers vortex (see e.g. Lautrup 2005) represents a viscous vortex flow with solid-body rotation and almost constant vorticity $\omega_z = a\Gamma/(4\pi\nu)$ near the axis of rotation; the flow gradually becomes potential with $\omega_z = 0$ at large distances. The vortex structure is qualitatively similar to that of the well-known Rankine vortex (Lamb 1932; Lautrup 2005) in a perfect fluid with a sharp interface between the vortex and potential flows at some arbitrary distance r_0. (Note that solution (10) is called the Rankine vortex in Odgaard 1986.)

The maximum azimuthal velocity for the solution (10) occurs at

$$r = r_c \quad \text{where} \quad r_c \equiv \sqrt{\frac{4\nu\vartheta}{a}} = \sqrt{\frac{4\pi\nu\vartheta H_0 r_0^2}{-Q}}, \tag{12}$$

and $\vartheta \approx 1.256$ is the root of the transcendental equation $2\vartheta = e^\vartheta - 1$. The parameter r_c determines the characteristic scale of the viscous vortex flow; beyond this distance, it rapidly reduces to the potential and inviscid flow. The maximum azimuthal velocity occurring at $r = r_c$ is given by:

$$(u_\varphi)_{max} = \frac{\Gamma}{2\pi r_c} \left(1 - e^{-\vartheta} \right). \tag{13}$$

The Burgers solution (10) is exact for an unbounded viscous fluid with linearly varying radial and axial components as represented by (7) and (8) (Lautrup 2005). However, with regard to the bathtub-vortex problem, this solution is valid only in the vicinity of the z-axis, where $r \leqslant r_0$, and for small whirlpool amplitude, $\eta \ll H_0$.

The pressure field consistent with the above solution may be readily determined by substitution of (7) and (8) into (2) and (4):

$$\frac{1}{\rho} \frac{\partial p}{\partial r} = \frac{\Gamma^2}{4\pi^2 r^3} \left[1 - \exp\left(-\frac{a}{4\nu} r^2 \right) \right]^2 - \frac{a^2}{4} r, \tag{14}$$

$$\frac{1}{\rho} \frac{\partial p}{\partial z} = -g - a^2 (z - H_0). \tag{15}$$

A formal solution to this set of equations can be presented in the form:

$$\frac{p}{\rho} = \frac{P_a - P_s}{\rho} + g\left(H_0 - z\right) - \frac{a^2}{2}\left[\frac{r^2}{4} + (z - H_0)^2 - H_0^2\right] - \frac{a\Gamma^2}{32\nu\pi^2}\int_{ar^2/2\nu}^{\infty}\left(\frac{1 - e^{-\varsigma}}{\varsigma}\right)^2 d\varsigma,$$

(16)

where P_a is the atmospheric pressure, and P_s is the pressure due to the surface tension. Note that the last two terms in this expression (both of which contain a) should be omitted for the large-r limit. They appear in the solution owing to the linear velocity fields described by (7) and (8), which are strictly valid only in the vicinity of the z-axis. When $r \to \infty$, both radial and vertical velocity components vanish and do not contribute to the total pressure. Accordingly, the pressure field in this asymptotic range is described by the hydrostatic formula: $p = P_a + \rho g\left(H_0 - z\right)$. The surface tension pressure also vanishes far from the z-axis as the free surface is assumed flat at infinity.

Following Odgaard (1986), we can estimate the condition for the existence of the critical vortex (i.e. the vortex whose gaseous core reaches the bottom orifice). At the centre of the critical-vortex tip, $r = z = 0$, the pressure is equal to the atmospheric pressure, hence (16) reduces to

$$\frac{P_s}{\rho} = gH_0 - \frac{aC\Gamma^2}{32\pi^2\nu} = gH_0 + \frac{CQ\Gamma^2}{32\pi^3\nu H_0 r_0^2},$$

(17)

where $C = \int_0^\infty (1 - e^{-\varsigma}/\varsigma)^2 d\varsigma \approx 1.385$. In general, the surface-tension pressure P_s depends on the free-surface curvature. The characteristic surface curvature produced by the whirlpool can be estimated as $\kappa \approx 2/r_c$ with r_c given by (12). Thus, the surface-tension pressure $P_s \approx -2\sigma/r_c$. Substituting this expression for P_s into (17), we obtain the equation relating the flow parameters in the critical regime of discharge:

$$H_0^2 = -\frac{\sigma}{\rho g r_0}\sqrt{-\frac{QH_0}{\pi\nu\vartheta}} - \frac{CQ\Gamma^2}{32\pi^3\nu g r_0^2}.$$

(18)

The same formula was derived by Odgaard (1986) through a slightly different consideration. When the surface tension is negligible ($\sigma = 0$), (18) reduces to

$$H_0 = \frac{\sqrt{C}}{4\pi}\frac{\Gamma}{r_0}\sqrt{\frac{-Q}{2\pi g\nu}} \quad \text{or equivalently} \quad \frac{Q}{\nu H_0} = -\frac{32\pi^3}{C}\left(\frac{H_0\sqrt{gH_0}}{\Gamma}\right)^2\left(\frac{r_0}{H_0}\right)^2.$$

(19)

This expression demonstrates that, in the critical regime of liquid discharge accompanied by vortex formation, the dimensionless drain rate (normalized by νH_0) depends not only on the ratio r_0/H_0, but also on the vortex intensity determined by the normalized circulation $\Gamma/H_0\sqrt{gH_0}$. This explains the experimental difficulty in measuring the critical liquid depth against the drain rate when the initial circulation in the liquid is unknown.

In another limiting case where strong surface tension predominates over the gravitation effect, an alternative expression can be obtained:

$$H_0 = -\frac{\vartheta Q}{4\pi\nu}\left(\frac{C\rho}{\sigma r_0}\right)^2\left(\frac{\Gamma}{4\pi}\right)^4 \quad \text{or} \quad \frac{Q}{\nu H_0} = -\frac{(4\pi)^5}{\vartheta C^2}\left(\frac{\sigma}{\rho g H_0^2}\right)^2\left(\frac{H_0\sqrt{gH_0}}{\Gamma}\right)^4\left(\frac{r_0}{H_0}\right)^2.$$

(20)

The derivation of (18) and its limiting cases, (19) and (20), are observed to be inconsistent as it has been assumed initially that the whirlpool dent is small in comparison with the total liquid depth and the equation for pressure (16) has therefore
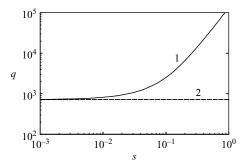
FIGURE 2. Dimensionless critical drain rate $q = |Q|\Gamma^2/(\nu g H_0^2 r_0^2)$ versus dimensionless surface tension $s = \sigma/(\rho\Gamma\sqrt{gH_0})$ (line 1) in the logarithmic scale. Line 2 shows the asymptotic value of the critical drain rate when the surface tension is negligible.

been applied beyond its formal range of validity. In reality, these equations represent rough estimates of the critical discharge regime. However, as will be shown below, the results obtained within the framework of this simplified approach are in a good qualitative, and reasonable quantitative, agreement with the more consistent theory.

Equation (18) can be expressed alternatively in terms of the dependence of a drain rate against liquid depth as:

$$\left(\frac{C}{32\pi^3}\frac{\Gamma^2}{gH_0^3}\right)^2\left(\frac{|Q|}{\nu H_0}\right)^2 - \left(\frac{r_0}{H_0}\right)^2\left[\frac{C}{16\pi^3}\frac{\Gamma^2}{gH_0^3} + \frac{1}{\pi\vartheta}\left(\frac{\sigma}{\rho gH_0^2}\right)^2\right]\frac{|Q|}{\nu H_0} + \left(\frac{r_0}{H_0}\right)^4 = 0. \tag{21}$$

Here, it can be ascertained that only one root of this equation is consistent with the limiting case of (20):

$$\frac{|Q|}{\nu H_0} = \frac{32\pi^3}{C}\frac{gH_0^3}{\Gamma^2}\left(\frac{r_0}{H_0}\right)^2$$

$$\times \left\{1 + \frac{16\pi^2}{\vartheta C}\frac{gH_0^3}{\Gamma^2}\left(\frac{\sigma}{\rho gH_0^2}\right)^2 + \sqrt{\left[1 + \frac{16\pi^2}{\vartheta C}\frac{gH_0^3}{\Gamma^2}\left(\frac{\sigma}{\rho gH_0^2}\right)^2\right]^2 - 1}\right\}. \tag{22}$$

The above equation can be written in a form containing only two dimensionless parameters, $q = |Q|\Gamma^2/(\nu g H_0^2 r_0^2)$ and $s = \sigma/(\rho\Gamma\sqrt{gH_0})$:

$$q = \frac{32\pi^3}{C}\left[1 + 2s\sqrt{\frac{8\pi^2}{\vartheta C}\left(1 + \frac{8\pi^2}{\vartheta C}s^2\right)} + \frac{16\pi^2}{\vartheta C}s^2\right]. \tag{23}$$

It follows from (22) that when the surface tension is negligible, the critical drain rate occurs such that the following combination of parameters is constant (cf. (19)): $|Q|\Gamma^2/(\nu g H_0^2 r_0^2) = 32\pi^3/C \approx 7.16 \times 10^2$. When the surface tension increases, the parameter q also increases, first linearly and then, in the limit of large s, quadratically, $q = (4\pi)^5 s^2/(\vartheta C^2)$; see figure 2. In this limit, (21) coincides with (20).

2.2. *More consistent consideration (the LABSRL-like model)*

For the construction of a more consistent theory, the approach developed by Lundgren (1985) and Andersen *et al.* (2003, 2006) will be adopted and developed further here without the assumption of uniform liquid rotation in the vessel (see also Lautrup, 2005). Consider a stationary whirlpool of arbitrary amplitude which is described by

function $H(r)$. The basic set of equations (1)–(4) are scaled by means of the following transformations:

$$\xi = r/H_0, \quad \zeta = z/H_0, \quad \{w_r, w_\varphi, w_z\} = \{u_r, u_\varphi, u_z\}/U_*, \quad P = p/(\rho U_*^2),$$
$$Re = H_0 U_*/\nu, \quad (24)$$

where $U_* = (gH_0)^{1/2}$ is the characteristic velocity. The parameter Re denotes the effective Reynolds number. By assuming w_r and w_φ to be independent of vertical coordinate ζ, the basic set of equations can be reduced to:

$$\frac{1}{\xi}\frac{d(\xi w_r)}{d\xi} + \frac{\partial w_z}{\partial \zeta} = 0, \quad (25)$$

$$w_r \frac{dw_r}{d\xi} - \frac{w_\varphi^2}{\xi} = -\frac{\partial P}{\partial \xi} + \frac{1}{Re}\frac{d}{d\xi}\left[\frac{1}{\xi}\frac{d(\xi w_r)}{d\xi}\right], \quad (26)$$

$$w_r = \frac{1}{Re}\frac{d}{d\xi}\ln\left[\frac{1}{\xi}\frac{d}{d\xi}(\xi w_\varphi)\right], \quad (27)$$

$$w_r\frac{\partial w_z}{\partial \xi} + w_z\frac{\partial w_z}{\partial \zeta} = -\frac{\partial P}{\partial \zeta} + \frac{1}{Re}\left(\frac{\partial^2 w_z}{\partial \xi^2} + \frac{1}{\xi}\frac{\partial w_z}{\partial \xi} + \frac{\partial^2 w_z}{\partial \zeta^2}\right) - 1. \quad (28)$$

Integrating (25) on ζ from 0 to $h(\xi) \equiv H(r/H_0)/H_0$, the following equation is obtained:

$$\frac{1}{\xi}\frac{d}{d\xi}(\xi w_r) + \frac{w_z(\xi, h) - w_z(\xi, 0)}{h(\xi)} = 0. \quad (29)$$

From the kinematic boundary condition on the free surface it follows $w_r(dh/d\xi) = w_z(\xi, h)$. Substituting this expression into (29) yields

$$\frac{d}{d\xi}(\xi w_r h) = \xi w_z(\xi, 0). \quad (30)$$

This equation can be readily integrated if the axial velocity component at the bottom, $\zeta = 0$, is specified. Let us assume for simplicity (although it is not essential) that the suction through the intake pipe is uniform (other possibilities are discussed in Lautrup 2005) i.e.

$$u_z(r, 0) = \begin{cases} -U_0 & 0 \leqslant r \leqslant r_0 \\ 0 & r > r_0 \end{cases} \quad \text{or} \quad w_z(\xi, 0) = \begin{cases} -U_0/U_* & 0 \leqslant \xi \leqslant R, \\ 0 & \xi > R, \end{cases} \quad (31)$$

where $R = r_0/H_0$. The velocity suction is related to the total drain rate as $U_0 = -Q/\pi r_0^2$. The use of drain rate rather than the suction velocity makes more sense in the following consideration. By integrating (30) with given velocity at the bottom (31), and assuming continuity of the radial velocity at $r = r_0$, the following expressions can be derived:

$$w_r h = -A \begin{cases} \xi, & 0 \leqslant \xi \leqslant R, \\ \dfrac{R^2}{\xi}, & \xi > R, \end{cases} \quad (32)$$

where $A = -Q/(2\pi r_0^2 U_*) > 0$. Under the above assumption that w_ξ and w_φ are independent of ζ, equations (26) and (28) can be presented by means of (25) in the

form of

$$\frac{\partial P}{\partial \xi} = -w_r \frac{dw_r}{d\xi} + \frac{w_\varphi^2}{\xi} + \frac{1}{Re} \frac{d}{d\xi} \left[\frac{1}{\xi} \frac{d(\xi w_r)}{d\xi} \right], \tag{33}$$

$$\frac{\partial P}{\partial \zeta} + 1 = \frac{w_z^2}{\xi} \frac{\partial}{\partial \xi} \left(\frac{\xi w_r}{w_z} \right) + \frac{1}{Re} \left(\frac{\partial^2 w_z}{\partial \xi^2} + \frac{1}{\xi} \frac{\partial w_z}{\partial \xi} + \frac{\partial^2 w_z}{\partial \zeta^2} \right). \tag{34}$$

Note that the right-hand side of (33) is not dependent on ζ, hence from the compatibility condition, $\partial^2 P/\partial \xi \partial \zeta = \partial^2 P/\partial \zeta \partial \xi$, it follows that the right-hand side of (34) is a function of ζ and can be denoted as $dF(\zeta)/d\zeta$. After integration on ζ, the pressure field can be determined through the formula

$$P = P_0 + h(\xi) - \zeta + F(\zeta) + P_s(\xi), \tag{35}$$

where P_0 is the normalized atmospheric pressure and $P_s(\xi)$ is the normalized pressure due to surface tension.

In the previous subsection, the surface tension pressure was estimated as $P_s \approx -2\sigma/r_c$. However, the free-surface curvature can be presented in an exact differential form, so that the surface tension pressure is given by (cf. Andersen *et al.* 2003, 2006):

$$P_s \equiv \frac{p_s}{\rho g H_0} = -\frac{\sigma}{\rho g H_0^2} \frac{1}{\xi} \frac{d}{d\xi} \frac{\xi(dh/d\xi)}{\sqrt{1 + (dh/d\xi)^2}}. \tag{36}$$

At infinity (large distances from the z-axis), the liquid is assumed to be at rest with a constant depth H_0, the free surface is flat (no curvature), and the pressure in the liquid varies in accordance with the hydrostatic formula; in dimensionless variables, the pressure is given by $P = P_0 + 1 - \zeta$. From this limiting case, it follows that $F(\zeta) = 0$. Substitution of (35) and (36) into (33) gives the following equation:

$$\frac{d}{d\xi} \left[h(\xi) - \frac{We^{-1}}{\xi} \frac{d}{d\xi} \frac{\xi(dh/d\xi)}{\sqrt{1 + (dh/d\xi)^2}} \right] - \frac{w_\varphi^2}{\xi} = \frac{d}{d\xi} \left[\frac{Re^{-1}}{\xi} \frac{d(\xi w_r)}{d\xi} - \frac{w_r^2}{2} \right], \tag{37}$$

where $We = \rho U_*^2 H_0 / \sigma$ is the Weber number comparing gravity to surface-tension effects.

Consider now the case of very large Reynolds numbers $Re \gg 1$. Following (27), $w_r \sim Re^{-1}$, both the terms in the right-hand side of (37) are of the order of Re^{-2}. They can thus be neglected in the first approximation. The truncated equation should be solved simultaneously with (27) and (32) resulting in the complete set of equations after elimination of w_r (cf. Andersen *et al.* 2003, 2006; Lautrup 2005):

$$h(\xi) \frac{d}{d\xi} \ln \left[\frac{1}{\xi} \frac{d(\xi w_\varphi)}{d\xi} \right] = -Q_R \xi \begin{cases} 1, & 0 \leqslant \xi \leqslant R, \\ \dfrac{R^2}{\xi^2}, & \xi > R, \end{cases} \tag{38}$$

$$\frac{d}{d\xi} \left[h(\xi) - \frac{We^{-1}}{\xi} \frac{d}{d\xi} \frac{\xi(dh/d\xi)}{\sqrt{1 + (dh/d\xi)^2}} \right] = \frac{w_\varphi^2}{\xi}, \tag{39}$$

where $Q_R \equiv A Re = (U_0/U_*)(Re/2) = |Q| H_0/(2\pi \nu r_0^2)$ is the normalized drain rate which determines the fluid flow together with two other dimensionless parameters, R and We.

These equations should be complemented by suitable boundary conditions. For conditions that are far from the z-axis ($\xi \to \infty$), all perturbations in the fluid are

expected to vanish, and the liquid depth approaches its equilibrium value, $h \to 1$ ($H \to H_0$ in the dimensional variables):

$$h(\infty) = 1, \quad \left.\frac{\mathrm{d}h}{\mathrm{d}\xi}\right|_{\xi=\infty} = 0, \quad \left.\frac{\mathrm{d}^2h}{\mathrm{d}\xi^2}\right|_{\xi=\infty} = 0, \quad w_\varphi(\infty) = 0, \quad \left.\frac{\mathrm{d}w_\varphi}{\mathrm{d}\xi}\right|_{\xi=\infty} = 0. \quad (40)$$

Another set of boundary conditions may be imposed at the axis of symmetry, $\xi = 0$. It is assumed that the azimuthal velocity at the axis vanishes; the depth of the whirlpool dent is maximal and the whirlpool shape is a smooth function of ξ so that the derivative $\mathrm{d}h/\mathrm{d}\xi$ also vanishes at $\xi = 0$. Three other parameters at $\xi = 0$, namely the liquid depth h_0, the curvature of the whirlpool profile h_0'', and the gradient of the azimuthal velocity component w_φ', can be considered as free parameters. Thus, the boundary conditions at $\xi = 0$ are:

$$h(0) = h_0, \quad \left.\frac{\mathrm{d}h}{\mathrm{d}\xi}\right|_{\xi=0} = 0, \quad \left.\frac{\mathrm{d}^2h}{\mathrm{d}\xi^2}\right|_{\xi=0} = h_0'', \quad w_\varphi(0) = 0, \quad \left.\frac{\mathrm{d}w_\varphi}{\mathrm{d}\xi}\right|_{\xi=0} = w_\varphi'. \quad (41)$$

There are therefore six parameters which determine the stationary whirlpool: Q_R, We, R, h_0, h_0'', and w_φ'. For given values of the external parameters that determine the global fluid flow (Q_R, We and R), the other three parameters determine the internal whirlpool structure, h_0, h_0'' and w_φ', and play an important role forming the 'eigenvalue vector' $\lambda = \{h_0, h_0'', w_\varphi'\}$. Physically acceptable solutions of the boundary-value problem (38)–(41) may exist only at certain values of λ. Such solutions are numerically constructed and discussed in the next section.

Note that, if the characteristic whirlpool width is much less than the radius of the discharge bottom orifice r_0, the parameter R becomes unimportant. The characteristic whirlpool width may be estimated from the analytical solution (10). In dimensionless variables, this solution becomes:

$$w_\varphi = \frac{K}{2\pi\xi}\left[1 - \exp\left(-\frac{Q_R}{2}\xi^2\right)\right], \quad (42)$$

where $K = \Gamma/(U_* H_0)$ is the Kolf number. The characteristic whirlpool width (i.e. the coordinate where the azimuthal velocity maximum occurs) is: $\xi_c \equiv r_c/H_0 = \sqrt{2\vartheta/Q_R}$ (cf. (12)). It follows that the radius of the outlet orifice becomes unimportant when $R \gg \xi_c$, and the whirlpool structure ceases to be dependent on R. From (42), we can readily estimate the azimuthal velocity gradient at $\xi = 0$ as:

$$w_\varphi' = \frac{KQ_R}{4\pi}. \quad (43)$$

The above expression assists in constructing a solution to the boundary-value problem (38)–(41).

Another useful parameter – the maximum value of the azimuthal velocity – can also be estimated from the approximate analytical solution (42):

$$w_{max} \equiv w_\varphi(\xi_c) = \frac{1 - \mathrm{e}^{-\vartheta}}{2\pi\sqrt{2\vartheta}}K\sqrt{Q_r}. \quad (44)$$

This parameter will be used for the comparison of approximate analytical solution against numerical results.

Note that substitution of (42) into (38) yields $h(\xi) = 1$. This reflects the approximate character of Odgaard's theory insofar as it is strictly valid only for relatively small-dent whirlpools: $\tilde{\eta} \equiv 1 - h_0 \ll 1$. A more consistent approximate expression for the

whirlpool profile can be obtained from (39) with the velocity profile described by (42). Neglecting the second term in the square brackets of (39) under the assumption $We \gg 1$, this equation can be integrated to yield:

$$h(\xi) \approx 1 - \int_\xi^\infty \frac{w_\varphi^2}{\xi'} \mathrm{d}\xi'. \tag{45}$$

Substitution of the velocity profile given by (42) into the integral (45) after simple manipulation gives:

$$h(\xi) \approx 1 - Q_R \left(\frac{K}{4\pi}\right)^2 \int_{Q_R\xi^2/2}^\infty \left(\frac{1-\mathrm{e}^{-z}}{z}\right)^2 \mathrm{d}z$$

$$= 1 - 2Q_R \left(\frac{K}{4\pi}\right)^2 \left[\mathrm{Ei}\left(-Q_R\xi^2\right) - \mathrm{Ei}\left(-\frac{Q_R\xi^2}{2}\right) + \frac{1}{Q_R\xi^2}\left(1 - \mathrm{e}^{-Q_R\xi^2/2}\right)^2\right], \tag{46}$$

where $\mathrm{Ei}(x)$ is the exponential integral (see e.g. the website http://mathworld. wolfram.com/ExponentialIntegral.html). Essentially the same solution has been obtained by Miles (1998) as the first-order Taylor series solution on the small parameter $\varepsilon \equiv Q_R K^2/(4\pi)^2 \ll 1$. In the zero-order approximation of this parameter (i.e. when $\varepsilon = 0$), solution (46) reduces to that obtained by Rott (1958) and Odgaard (1986).

The approximate analytical formula for the whirlpool shape is derived when surface tension is neglected. Correcting this formula for the effect of surface tension has been performed in a separate paper (Stepanyants & Yeoh 2008). Strictly speaking, the formula is valid only for whirlpools of small amplitude as it is based on the application of (42) which was obtained under this same assumption. The analysis of (46) and its comparison with the results of numerical solutions of the boundary-value problem (38)–(41) will be discussed in the next section.

3. Numerical solutions of the boundary-value problem for stationary whirlpools

The boundary-value problem (38)–(41) has been studied numerically for two cases: (i) whirlpools without surface tension and (ii) with surface tension. The first case is relatively simple because the set of equations (38), (39) with $We \to \infty$ reduces to only three first-order ordinary differential equations (ODE) with the following boundary conditions:

$$h(\infty) = 1, \quad w_\varphi(\infty) = 0, \quad \left.\frac{\mathrm{d}w_\varphi}{\mathrm{d}\xi}\right|_{\xi=\infty} = 0, \tag{47}$$

$$h(0) = h_0, \quad w_\varphi(0) = 0, \quad \left.\frac{\mathrm{d}w_\varphi}{\mathrm{d}\xi}\right|_{\xi=0} = w_\varphi'. \tag{48}$$

The number of independent free parameters reduces to four in this case: Q_R, R, h_0 and w_φ'.

3.1. *Stationary whirlpools without surface tension*

The boundary-value problem (38)–(41) with $We \to \infty$ and fixed values of Q_R and R has been numerically integrated by the use of the Mathcad software. Several different numerical algorithms have been exploited to solve the ODEs (such as the
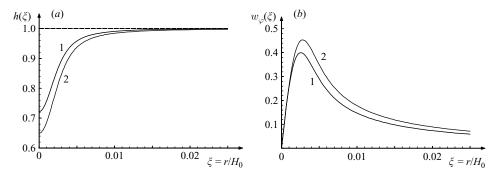
FIGURE 3. Subcritical whirlpool: (a) free surface; (b) azimuthal velocity component for $R = 0.05$, $Q_R = 3.18 \times 10^5$ and $K = 1.12 \times 10^{-2}$. Lines: 1, the numerical solution; 2, the approximate analytical solutions for the free surface (46) and azimuthal velocity (42). The dimensionless liquid depth at the whirlpool tip is $h_0 = 0.7222$ (the depth of whirlpool dent is $\tilde{\eta} = 0.2778$). The velocity gradient, w'_φ, was chosen in accordance with (43).

fourth-order Runge–Kutta methods with fixed and adaptive steps, as well as the Bulirsch–Stoer method). All available algorithms that have been tested have yielded essentially identical results.

The first result is shown in figure 3 for the particular values of parameters indicated in the figure caption. The approximate analytical solutions for the whirlpool shape, (46), and velocity profile, (42), are also shown. Good qualitative and even quantitative agreement between the approximate analytical and numerical solutions can be seen. The agreement becomes even better when the depth of whirlpool dent decreases. For whirlpools of very small dent (i.e. when $\tilde{\eta} \ll 1$), the analytical and numerical solutions become indistinguishable.

The characteristic whirlpool size shown in figure 3 is $\xi_c \sim 2.8 \times 10^{-3} \ll R = 0.05$. This means that the whirlpool is concentrated entirely within the water column above the bottom orifice, and the parameter R is irrelevant in this case.

The radial velocity component, w_r, readily follows from (32) and is shown in figure 4(a). The axial velocity component, w_z, is determined from (25) and (31):

$$w_z(\xi, \zeta) = \begin{cases} -2A - \dfrac{\zeta}{\xi} \dfrac{\mathrm{d}(\xi w_r)}{\mathrm{d}\xi}, & 0 \leqslant \xi \leqslant R, \\ 0, & \xi > R. \end{cases} \qquad (49)$$

Figure 4(b) illustrates the dependence of w_z on ξ for several value of ζ. As seen from figure 4, the profiles of both the radial and axial velocity components are in accordance with the assumptions made in the simplified theory, (7) and (8), at least for whirlpools of moderate amplitudes.

In the vicinity of the vortex tip, the Taylor series expansion of $h(\xi)$ and $w_\varphi(\xi)$ can be constructed yielding:

$$h(\xi) = h_0 + \frac{(w'_\varphi)^2}{2}\xi^2 - \frac{(w'_\varphi)^2 Q_R}{8h_0}\xi^4 + \frac{(w'_\varphi)^2 Q_R}{288h_0^2}[7Q_R + 4(w'_\varphi)^2]\xi^6 - \cdots, \quad (50a)$$

$$w_\varphi(\xi) = w'_\varphi \xi \left\{ 1 - \frac{Q_R}{4h_0}\xi^2 + \frac{Q_R}{24h_0^2}[Q_R + (w'_\varphi)^2]\xi^4 - \cdots \right\}. \qquad (50b)$$

It is clear that the solution becomes singular when $h_0 = 0$. It can be readily proved that there are no power-type solutions in the forms of $h(\xi) \sim \xi^\alpha$ and $w_\varphi(\xi) \sim \xi^\beta$ in

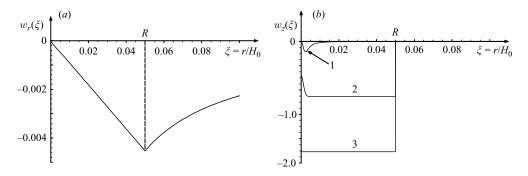FIGURE 4. Radial (*a*) and axial (*b*) velocity components for the subcritical whirlpool shown in figure 3(*b*). Line 1 corresponds to the free surface $\zeta = h(\xi)$; line 2 to $\zeta = 0.5$; and line 3 to $\zeta = 0$ (the bottom level).
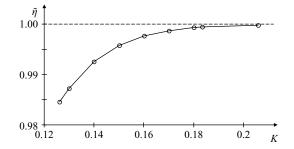

FIGURE 5. Dependence of the dimensionless depth of whirlpool dent, $\tilde{\eta} \equiv 1 - h_0$, on Kolf number $K = \Gamma/(U_* H_0)$ (circles represent the computed values connected by straight lines). The parameter $Q_R = 5 \times 10^4$ is fixed, and the velocity gradient was chosen in accordance with the (43).

the leading order on ξ when $h_0 = 0$. Aforementioned numerical algorithms are also unable to provide a direct numerical solution of the boundary-value problem in this particular case.

However, by systematically adjusting the Kolf number K with fixed parameter Q_R, it is possible to approach the 'near-critical' whirlpool for which h_0 is very close but not equal to zero. Figure 5 shows the near-critical situation when $Q_R = 5 \times 10^4$. The liquid depth at the whirlpool centre in this case is $h_0 = 10^{-4}$ (the whirlpool amplitude is $\tilde{\eta} = 0.9999$) when $K = 0.206$. The shape of the 'near-critical whirlpool' with the parameter values indicated above is shown in figure 6(*a*). The comparison of the numerically calculated azimuthal velocity profile with the approximate analytical solution (42) is shown in figure 6(*b*). It is clear from figure 6(*b*) that the discrepancy between the numerical and approximate analytical solution (42) is significant, although the asymptotic behaviour is the same as $\xi \to 0$. The radial and axial velocity components for this case are shown in figure 7.

Choosing the value of $h_0 = 10^{-4}$ as the condition for a threshold below which the gas entrainment into the drainage pipe may occur, the dependence between the parameters Q_R and K can be established for the 'near-critical' whirlpools. This dependence has been obtained from the result of calculations of the boundary-value problem (38), (39) and (47), (48) and is shown in figure 8. The best fit approximation
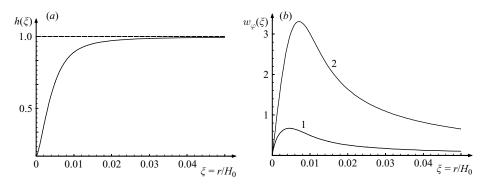
FIGURE 6. The 'near-critical' whirlpool: (*a*) free surface; (*b*) azimuthal velocity component for $R = 0.05$, $Q_R = 5 \times 10^4$ and $K = 0.206$. (*b*) Line 1 represents the numerical solution, and line 2 the approximate analytical solution (42). The dimensionless liquid depth at the whirlpool tip is $h_0 = 0.0001$ (the depth of whirlpool dent is $\tilde{\eta} = 0.9999$), and the velocity gradient, w'_φ, was chosen in accordance with the (43).
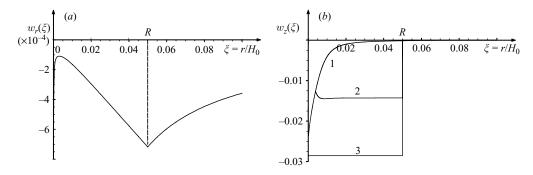

FIGURE 7. Radial (*a*) and axial (*b*) velocity components for the 'near-critical' whirlpool shown in figure 6(*b*). Line 1 corresponds to the free surface $\zeta = h(\xi)$; line 2 to $\zeta = 0.5$; and line 3 to $\zeta = 0$ (the bottom level).

of the numerical results gives

$$K = 46.154\, Q_R^{-1/2} \quad \text{or in the dimensional form} \quad H_0 = \frac{1}{46.154} \frac{\Gamma}{r_0} \sqrt{\frac{-Q}{2\pi g \nu}}. \quad (51)$$

The above formula can be compared with what follows from (46) for the critical vortex. When $h_0 = 0$ (the condition of the critical vortex), (46) provides exactly the same dependence $K = 4\pi/(C Q_R)^{1/2}$ as (19). It is observed that expressions (19) and (51) are the same apart from the numerical coefficient; namely, in the dimensional form, the coefficient δ is $1/46.154 \approx 0.022$ in (51) compared with $\delta = \sqrt{C}/(4\pi) \approx 0.094$ in (19). The same functional dependence, but again with different numerical coefficients, also follows from the empirical approach developed by Hite & Mih (1994) ($\delta = (1 - e^{-\vartheta})/(2\pi\sqrt{\vartheta}) \approx 0.102$) and from the estimate by Lautrup (2005) ($\delta = 1/(2\pi) \approx 0.16$, see (26–52) in his book for the case $h_0 = 0$).

The approximate estimates from Odgaard (1986) and Lautrup (2005), the empirical approach of Hite & Mih (1994) based on the processing of experimental data, as well as the results of our numerical calculations with a LABSRL-like model, all predict the same functional dependence of flow parameters for the critical whirlpool when surface tension is neglected. The only difference is in terms of the parameter q as defined
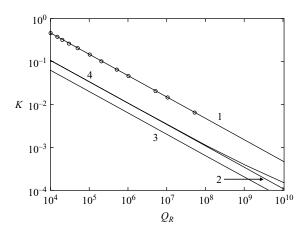
FIGURE 8. Dependence of Kolf number K on $Q_R = |Q|H_0/(2\pi\nu r_0^2)$ in the logarithmic scale. Circles are the results of numerical calculations without surface tension; line 1 is the best fit approximation to the numerical data as given by (50) $K = 46.154 Q_R^{-1/2}$; line 2 is the dependence $K = 4\pi (C Q_R)^{-1/2}$ that follows from (19) where the surface tension is neglected; line 3 is the dependence $K = 2\pi Q_R^{-1/2}$ that follows from Lautrup (2005); line 4 is the dependence that follows from (54) when the surface tension is taken into account.

above (23): $q = (2\pi)^3 \approx 2.48 \times 10^2$ from Lautrup's estimate; $q = (2\pi)^3 \vartheta/(1 - e^{-\vartheta})^2 \approx 6.09 \times 10^2$ from Hite & Mih's (1994) empirical approach; $q \approx 7.16 \times 10^2$ from Odgaard's approximate theory; and $q \approx 1.34 \times 10^4$ from our calculations.

The theoretical model that has been developed in §2.2 also permits a numerical study of the supercritical drainage regime. This situation arises when the bathtub vortex is of such intensity that it results in the entrainment of a gaseous core into the intake pipe. Numerical solutions of the boundary-value problem (38)–(39), (47)–(48) have been successfully obtained for this case by formally assigning some negative values for h_0. The larger the negative value h_0, the thicker is the vortex gaseous core. Note that the suction velocity through the output orifice cannot be assumed uniform as was the case in (31). However, the structure of the whirlpool is practically insensitive to the velocity distribution through the orifice; it depends only on the total drain-rate value.

An example of a supercritical whirlpool is shown in figures 9 and 10. For the parameter values chosen, the viscous vortex scale (see (42)) is $\xi_c \approx 7 \times 10^{-3}$, whereas the air core radius amounts to $\xi_a = 5 \times 10^{-3}$. Such a vortex lies almost entirely in the potential flow domain where the azimuthal velocity $w_\varphi \sim \xi^{-1}$. This dependence is in good agreement with our numerical calculation shown in figure 9(b).

Stationary supercritical vortices have been studied numerically by Forbes & Hocking (1995) within the framework of a primitive set of hydrodynamic equations of an ideal fluid without surface tension. Our results are found to be qualitatively similar to those obtained by these authors.

3.2. *Influence of surface tension on the structure of stationary whirlpools*

Under certain conditions, surface tension may affect the whirlpool shape. The condition where the surface tension becomes important follows from a comparison of the characteristic whirlpool size r_c (see (12)) and the capillary scale $l_{cap} \sim (\sigma/\rho g)^{1/2}$ (for water flow $l_{cap} \approx 0.27$ cm) (see e.g. Andersen *et al.* 2006). For whirlpools with
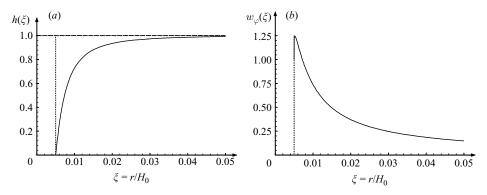
FIGURE 9. Supercritical whirlpool: (*a*) free surface; (*b*) azimuthal velocity component for $R = 0.05$, $Q_R = 5 \times 10^4$ and $K = 0.000991$. The dotted vertical lines designate the width of the air core.
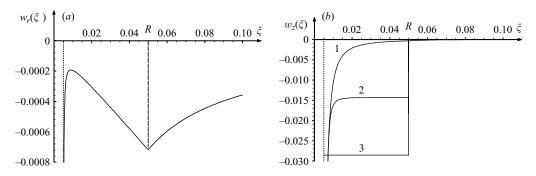

FIGURE 10. Radial (*a*) and axial (*b*) velocity components for the supercritical whirlpool shown in figure 9. (*b*) Line 1 corresponds to the free surface $\zeta = h(\xi)$; line 2 to $\zeta = 0.5$; and line 3 to $\zeta = 0$ (the bottom level).

$r_c \leqslant l_{cap}$ the surface tension cannot be neglected. This condition yields:

$$H_0 \leqslant \frac{\sigma}{4\vartheta \rho g \nu} U_0 \quad \text{or in the dimensionless form} \quad We \leqslant Q_R/(2\vartheta). \tag{52}$$

From above, the liquid depth for vortices that are affected by surface tension is proportional to the drainage rate. The coefficient of proportionality thus depends only on the liquid properties. In particular, for water flow, condition (50) results in $H_0(\text{m}) \leqslant 1.64 \, U_0 \, (\text{m s}^{-1})$, and for $U_0 = 1 \, \text{m s}^{-1}$, the liquid depth must be $H_0 \leqslant 1.64 \, \text{m}$. Note that the depth of whirlpool dent may be much smaller than H_0.

To determine the influence of surface tension on whirlpool shape and amplitude, the boundary-value problem represented by (38)–(41) should be considered. This, however, requires the evaluation of another component of the eigenvalue vector λ, which is the parameter h_0'' – the free surface curvature at the whirlpool tip. The complexity of the problem increases significantly when this parameter is taken into consideration.

For a particular set of eigenvalue components, the boundary-value problem has been numerically solved for fixed values of external parameters Q_R, We and K. The surface tension effect yields a shallower whirlpool dent in comparison with the case of surface tension being ignored (cf. Andersen *et al.* 2003, 2006). Typical computational results are shown in figures 11 and 12 for $R = 0.05$, $Q_R = 10^6$, $We = 3.4 \times 10^4$, and
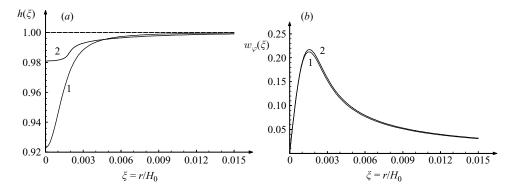
FIGURE 11. Typical whirlpool shapes (*a*) and azimuthal velocities (*b*) without (line 1) and with (line 2) surface tension. For the given external flow parameters (see text), the water depths at the whirlpool tip are: for the case without surface tension $h_0 = 0.923$ ($\tilde{\eta} = 0.077$); for the case with surface tension $h_0 = 0.981$ ($\tilde{\eta} = 0.019$). Only the portion of the ξ-axis interval is shown, $0 \leqslant \xi \leqslant 0.3R$.
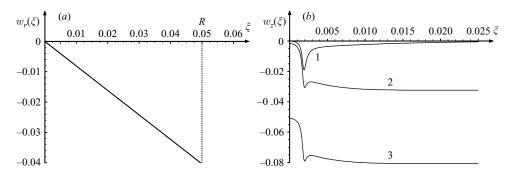

FIGURE 12. Radial (*a*) and axial (*b*) velocity components for the subcritical whirlpool with surface tension shown in figure 11 (note that both horizontal and vertical scales are different in (*a*) and (*b*)). (*b*) Line 1 corresponds to the free surface $\zeta = h(\xi)$; line 2 to $\zeta = 0.98$; and line 3 to $\zeta = 0.95$. The axial velocity within the outlet orifice, $0 \leqslant \xi \leqslant R$, is constant and amounts to -1.614.

$K = 3.05 \times 10^{-3}$. In spite of the significant difference in the whirlpool shape and depth, its velocity field, nevertheless, remains only marginally affected by the surface tension, as seen in figure 11(*b*) where the azimuthal velocity profiles are shown. The negligible effect of surface tension on the azimuthal velocity also prevails for the radial and axial velocities; the corresponding velocity profiles for the whirlpools with and without surface tension are indistinguishable for the above parameter set.

When surface tension is accounted for, numerical solutions have been obtained for whirlpools of relatively small dent, $\eta < 0.03 \, H_0$. However, all attempts to construct numerical solutions for whirlpools of larger depression have been unsuccessful. It is not clear whether this has been caused by the difficulty of choosing a relevant multi-component vector eigenvalue or by the non-existence of stationary vortices at large dents. There is some numerical and experimental evidence indicating that large-dent vortices tend to become unstable; they oscillate vertically, bend and 'dance' around the central axis, lose air bubbles which are subsequently drawn into the drainage pipe (see e.g. Andersen *et al.* 2006, figure 3). In this situation, the influence of surface

tension on the whirlpool dip, especially for critical vortices, can be only roughly estimated.

By integrating (39) on ξ from 0 to infinity and taking into account that the free-surface curvature at $\xi = 0$ is $\kappa(0) = h_0''$, whereas at infinity where the surface is flat, it is zero, the vortex amplitude can be determined as:

$$\tilde{\eta} = \int_0^\infty \frac{w_\varphi^2}{\xi} \, d\xi - \frac{h_0''}{We}. \tag{53}$$

It follows from this equation that the whirlpool amplitude becomes smaller when the Weber number is finite (it is obvious that $h_0'' > 0$ for the concave surface due to a whirlpool) provided that the azimuthal velocity field is not greatly influenced by the surface-tension effect. This is the case at least for vortices of relatively small dips (see figure 12*b*).

For the critical whirlpool with $h_0 = 0$, the integral in (53) can be estimated on the basis of the approximate analytical solution (42), and the surface curvature in the whirlpool tip can be estimated as $\kappa(0) \sim 2/\xi_c$, where ξ_c is the characteristic dimensionless whirlpool width (see the expression for ξ_c after (42)). Substituting these factors into (53) with $\eta = 1$ yields exactly the same expression as that obtained from Odgaard's model (cf. (18) in dimensional variables):

$$K = \frac{4\pi}{\sqrt{CQ_R}} \sqrt{1 + \frac{1}{We} \sqrt{\frac{2Q_R}{\vartheta}}}. \tag{54}$$

This dependence is shown in figure 8 by line 4. As follows from (54), the influence of surface tension becomes noticeable only for very high values of Q_R or small values of We. For the purposes of illustration, line 4 in figure 8 is plotted for $We = 7.36 \times 10^{-6}$ which corresponds to the air–water interface at $T = 25°C$ and $H_0 = 1$ m.

Equation (54) allows us to estimate the condition where the surface tension affects the critical vortex:

$$We \leqslant \sqrt{\frac{2Q_R}{\vartheta}} \quad \text{or} \quad H_0 \leqslant \left(\frac{U_0 \sigma^2}{\vartheta \nu \rho^2 g^2} \right)^{1/3} \tag{55}$$

This condition can be written in the form $r_c/l_{cap} \leqslant 2l_{cap}/H_0$. As the capillary scale l_{cap} is usually very small in comparison with the liquid depth, the last condition is much stronger than that given by (52). Substituting again the water parameters in (55), we obtain $H_0 \, (\text{m}) \leqslant 0.036 \, U_0^{1/3}$, where the flow velocity is in m s^{-1}. In particular, $H_0 \leqslant 3.6$ cm for $U_0 = 1$ m s^{-1} and increases very slowly with U_0. Both conditions (52) and (55) become equal for $U_0 = 8\vartheta \nu \sqrt{\rho g / \sigma}$ which for water flow gives $U_0 = 3.3$ mm s^{-1} and for the critical vortex dip $\eta = H_0 = 5.4$ mm.

In the derivation of (54), a simple estimation of the whirlpool curvature has been used $\kappa(0) \sim 2/\xi_c$. However, another estimation can be obtained from (39). Neglecting at large We the second term in the square brackets which is of the order of We^{-1}, and differentiating this equation once more, the relationship between the surface curvature and velocity field can be obtained as $h_0'' = [d(w_\varphi^2/\xi)/d\xi]|_{\xi=0}$. Using the approximate analytical expression for the azimuthal velocity, (42), we obtain $h_0'' = (KQ_R/4\pi)^2$. Then from (53), it follows that for the critical vortex with $\eta = 1$:

$$K = \frac{4\pi}{\sqrt{CQ_R \left(1 - \frac{Q_R}{CWe} \right)}}, \tag{56}$$
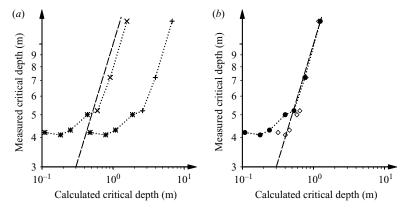
FIGURE 13. Measured versus calculated critical depth. Dashed lines show 100% correlation. Data obtained with molecular viscosity (connected for clarity by dotted lines) are shown in (*a*) by + (from Odgaard's formula (19)) and × (from our (51)). Asterisks indicate those data which noticeably deviate from the predicted functional dependences. Corrected data obtained with the appropriate eddy viscosity are shown in (*b*) by ◇ (from (19)) and by circles (from (51)).

where the constant C is that given after (17). This expression becomes singular when $We = Q_R/C$. In the dimensional form, the condition of singularity is met when $U_0 = 2C\rho vg H_0/\sigma$. For water flow this implies $U_0 = 0.34 H_0$ and, thus thus, for $H_0 = 1$ m, the critical vortex does not exist if $U_0 \geqslant 0.34$ m s^{-1}.

4. Experimental validation of results obtained

Andersen *et al.* (2003, 2006) obtained a very good correlation between the theoretical/numerical results within the framework of LABSRL-model with surface tension and their experimental data for the whirlpool shape and azimuthal velocity profile in a rotating container. However, good agreement was only achieved over a limited range of parameters (the rotation rate of the container and flow rate of water through it) with an appropriate choice of some fitting parameters. Critical whirlpools were not assessed in those papers.

The critical regime of discharge has been studied by several authors (see e.g. Jain, Raju & Garde 1978; Odgaard 1986; Kim 1994, and references therein). The comparison of results obtained from Odgaard's model and from our numerical calculations with the experimental data available from Odgaard (1986) is presented in figure 13. Both Odgaard's and our calculated data are based on laminar theory with the molecular viscosity of the liquid. The character of the dependence (i.e. the slopes of the dotted lines in the logarithmic scale) is the same for both models when the critical depth is sufficiently high, $H_0 > 0.5$ m, with only a parallel shift between Odgaard's and our results. Meanwhile, our results are noticeably closer to the 100% correlation straight line.

Both Odgaard's and our data deviate from perfect correlation when the critical depth is small, $H_0 < 0.5$ m. One possible explanation for this discrepancy between the theory and experiment may be associated with the influence of turbulence since the theory is based on the assumption of laminar flow. Some authors (see e.g. Einstein & Li 1955; Odgaard 1986; Hite & Mih 1994) have suggested the possible inclusion of a turbulent character of liquid motion at high Reynolds numbers into the model to accommodate the necessary flow physics. According to the semi-empirical approach,

the effect of small-scale turbulence may be incorporated within an effective viscosity ν_{eff}, whereas the expressions for the average hydrodynamic fields remain the same as those based on laminar theory. Using the eddy-viscosity concept, the effective viscosity can be taken as the sum of the molecular and eddy viscosities, $\nu_{eff} = \nu + \nu_{ed}$, where the eddy viscosity is proportional to the circulation $\nu_{ed} = k\Gamma$.

By imposing a value of $k = 6 \times 10^{-5}$, Odgaard (1986) obtained good agreement between his approximate theory and all experimental data (see diamonds in figure 13). The effective viscosity in his case varied in the range $\nu_{eff} = 2 \times 10^{-6} - 2.9 \times 10^{-5}$ m^2 s^{-1}, whereas water molecular viscosity is $\nu = 8.94 \times 10^{-7}$ m^2 s^{-1}.

By adopting a similar approach with a value of $k = 1.09 \times 10^{-6}$ ($\nu_{eff} = 9.14 \times 10^{-7} - 1.41 \times 10^{-6}$ m^2 s^{-1}), we also obtain excellent correlation between our results and experimental data for large critical depths (see circles in figure 13), whereas for small depths there is no significant improvement with the inclusion of eddy viscosity.

5. Conclusion

A theoretical model for stationary whirlpools has been constructed for a horizontally unbounded viscous liquid with a free surface. The development of the present model is found to be rather similar to those derived earlier by Lundgren (1985) and Anderson *et al.* (2003, 2006) who considered, however, the vortices in a rotating vessel. Qualitatively, our results are in good agreement with the approximate and rather inconsistent theory of Odgaard (1986).

For simplicity, the viscous models studied here and in the aforementioned papers have concentrated primarily on laminar flows. Applicability of such models is thus restricted by relatively low Reynolds numbers $Re \leqslant 2.3 \times 10^3$. In reality, Reynolds numbers for bathtub vortices generally exceed this threshold value even in laboratory experiments. However, the choice of parameters required to appropriately define the Reynolds number, especially for vortex flows, is not obvious. According to the formal definition of the effective Reynolds number used in the present paper, (24), the limitation on Reynolds number results in the restriction on the liquid height, $H_0 \leqslant 10^2 \, (\nu^2/g)^{1/3}$. For water flow, this yields $H_0 \leqslant 0.43$ m. On the other hand, the physical Reynolds number may be defined on the basis of whirlpool parameters using (12) and (13): $Re_w = r_c(u_\varphi)_{max}/\nu = \Gamma(1 - e^{-\vartheta})/(2\pi\nu)$ From the above criterion, it follows that a condition for water circulation in a whirlpool is: $\Gamma \leqslant 1.8 \times 10^{-2}$ m^2 s^{-1}.

Also it appears that the critical Reynolds number determining the transition to turbulent flow may be even higher than the above value of $Re = 2.3 \times 10^3$ obtained for Hagen–Poiseuille flow in a circular pipe. One plausible explanation is the suppression of the turbulence in swirling flows of vortex cores (a similar turbulent suppression effect is well known in a density stratified fluid).

The simplest correction to the laminar theory for supercritical Reynolds numbers may be performed by replacing the molecular viscosity of the liquid with the effective viscosity, which comprises the sum of the molecular and eddy viscosities. The latter may be several orders of magnitude greater than the former (see e.g. Einstein & Li 1955; Odgaard 1986). There is no theoretical basis for the inclusion of an eddy viscosity from first principles. This parameter, as it stands, is considered either as empirically obtained through a number of independent experimental data or as a fitting parameter assisting with the best fit of theory and experiment. (An interesting finding for the optimum eddy viscosity by Brocard *et al.* 1982 is mentioned in Hite & Mih 1994). A more in-depth investigation on this particular aspect is required.

Three different regimes of drainage have been studied in this paper: (i) subcritical – where the whirlpool dent is less than the fluid depth; (ii) critical – where the whirlpool bottom touches the bottom orifice; and (iii) supercritical – where the fluid discharge is accompanied by the formation of a gaseous core which penetrates into the outlet pipe. A relationship between flow parameters and liquid discharge has been established, in particular in the critical discharge regime. The vortices in the supercritical regime are similar to those which were numerically studied earlier by Forbes & Hocking (1995) within the framework of a primitive set of hydrodynamic equations for an ideal fluid without surface tension.

The influence of surface tension on whirlpool structure for the subcritical regime has been investigated. It has been confirmed that whirlpools of small dips are shallower for the same flow parameters if the effect of surface tension is taken into account (cf. Andersen *et al.* 2003, 2006). Nothing certain can be said so far about the influence of surface tension on large-dip vortices. Some speculative estimates obtained in §3.2 for critical vortices must be numerically and experimentally validated. This presents a challenge for future study.

Some other issues also remain outstanding. In particular, the influence of a second-order effect on the inverse Reynolds number, Re^{-2}, should be investigated. The model derived here can be further modified by replacing (39) with the more precise form of (37) augmented by (27). This, however, results in an increase in the order of ODEs with two additional components appearing in the eigenvalue vector $\boldsymbol{\lambda}$, namely w_φ'' and w_φ'''. The model would become rather complex, thus leaving as the only feasible option the construction of a numerical solution for whirlpools within the framework of a primitive set of hydrodynamic equations with viscosity and surface tension. Determining suitable eigenvalues represents a difficult and challenging task, which will be further explored in future studies.

REFERENCES

ANDERSEN, A., BOHR, T., STENUM, B., RASMUSSEN, J. J. & LAUTRUP, B. 2003 Anatomy of a bathtub vortex. *Phys. Rev. Lett.* **91**, 104502.

ANDERSEN, A., BOHR, T., STENUM, B., RASMUSSEN, J. J. & LAUTRUP, B. 2006 The bathtub vortex in a rotating container. *J. Fluid Mech.* **556**, 121–146.

ANDRADE, E. N. DA C. 1963 Whirlpools, vortices and bath tubs. *New Sci.* **17**, 302–304.

BAUM, M. R. 1974 Gas entrainment at the free surface of a liquid: entrainment inception at a laminar vortex. *J. Brit. Nucl. Engng Soc.* **13**, 203–209.

BINNIE, A. M. 1964 Some experiments on the bath-tub vortex. *J. Mech. Engng Sci.* **6**, 256–257.

CHANG, K. S. & LEE, D. J. 1995 An experimental investigation of the air entrainment in the shutdown cooling system during mid-loop operation. *Ann. Nucl. Energy* **22**, 611–619.

EINSTEIN, H. A. & LI, H. 1955 Steady vortex flow in a real fluid. *La Houille Blanche* **10**, 483–496.

FORBES, L. K. & HOCKING, G. C. 1995 The bath-plug vortex. *J. Fluid Mech.* **284**, 43–62.

GULLIVER, J. S., PAUL, T. C. & ODGAARD, A. J. 1988 *J. Hydraul. Engng ASCE* **114**, 447–452.

HECKER, G. E. 1981 Model-prototype comparison of free surface vortices. *J. Hydrol. Div. ASCE* **7** (HY10), 1243–1259.

HITE, J. E. & MIH, W. C. 1994 Velocity of air-core vortices at hydraulic intakes. *J. Hydraul. Engng ASCE* **120**, 284–297.

JAIN, A. K., RAJU, K. G. R. & GARDE, R. J. 1978 Vortex formation at vertical pipe intakes. *J. Hydrol. Div. ASCE* **104** (HY10), 1429–1445.

KELLY, D. L., MARTIN, B. W. & TAYLOR, E. S. 1964 A further note on the bathtub vortex. *J. Fluid Mech.* **19**, 539–542.

KIM, S.-N. 1994 A study on the free surface vortex in a pipe system. *The 4th Intl Topical Meeting on Nuclear Thermal Hydrulics, Operations and Safety, Taipei, Taiwan*, pp. 23-B-1–23-B-6.

KOCABAŞ, F. & YILDRIM, N. 2002 Effect of circulation on critical submergence of an intake pipe. *J. Hydraul. Res.* **40**, 741–752.

KNAUSS, J. 1987 Swirling flow problems at intakes. *Hydraulic Structure Design Manual.* Balkema.

LAMB, H. 1932 *Hydrodynamics*, 6th edn. Cambridge University Press.

LAUTRUP, B. 2005 *Physics of Continuous Matter: Exotic and Everyday Phenomena in the Macroscopic World.* IoP Publishing.

LUBIN, B. T. & SPRINGER, G. S. 1967 The formation of a dip on the surface of a liquid draining from a tank. *J. Fluid Mech.* **29**, 385–390.

LUGT, H. J. 1983 *Vortex Flow in Nature and Technology.* J. Wiley.

LUNDGREN, T. S. 1985 The vertical flow above the drain-hole in a rotating vessel. *J. Fluid Mech.* **155**, 381–412.

MARRIS, A. W. 1966 Theory of the bathtub vortex. *J. Appl. Mech., Trans. ASME*, 66-WA/APM-11.

MILES, J. 1998 A note on the Burgers–Rott vortex with a free surface. *Z. Angew. Math. Phys.* **49**, 162–165.

MONJI, H., AKIMOTO, T., MIWA, D. & KAMIDE, H. 2005 Behavior of free surface vortices in cylindrical vessel under fluctuating flow rate. In *The 11th Int. Topical Meeting on Nuclear Reactor Thermal-Hydraulics (NURETH-11), Avignon, France.*

ODGAARD, A. J. 1986 Free-surface air core vortex. *J. Hydraul. Engng ASCE* **112**, 610–620.

ROTT, N. 1958 On the viscous core of a line vortex. *Z. Angew Math. Phys.* **9b**, 543–553.

SIBULKIN, M. 1962 A note on the bathtub vortex. *J. Fluid Mech.* **14**, 21–24.

SIBULKIN, M. 1983 A note on the bathtub vortex and the Earth's rotation. *Am. Sci.* **71**, 352–353.

SHAPIRO, A. H. 1962 Buth-tub vortex. *Nature* **196**, 1080–1081.

STEPANYANTS, Y. A. & YEOH, G. H. 2008 Burgers–Rott vortices with surface tension. *J. Angew Math. Phys.* **59**, 1–12.

TREFETHEN, L., BILGER, R. W., FINK, P. T., LUXTON, R. E. & TANNER, R. I. 1965 The buth-tub vortex in the Southern hemisphere. *Nature* **207**, 1084–1085.

TURMLITZ, O. 1908 Ein neuerphysikalischer Beweis der Achsendrehung der Erde. *S.B. Akad. Wiss. Wien, Abt. IIa.* **117**, 819.

TYVAND, P. A. & HAUGEN, K. B. 2005 An impulsive bathtub vortex. *Phys. Fluids* **17**, 062105.

ZHOU, Q.-N. & GRAEBEL, W. P. 1990 Axisymmetric drainage of a cylindrical tank with a free surface. *J. Fluid Mech.* **221**, 511–532.